DOI: 10.1002/ ((please add manuscript number))

Article type: Full paper

Redox-stability of alkoxy-BDT copolymers and their use for organic bioelectronic devices

Alexander Giovannitti, Karl J. Thorley, Christian B. Nielsen, Jun Li, Mary J. Donahue, George G. Malliaras, Jonathan Rivnay and Iain McCulloch*

Dr. A.Giovannitti, Dr. K. J. Thorley, Dr. J. Li, Prof. I. McCulloch
Department of Chemistry and Centre for Plastic Electronics
Imperial College London
Exhibition Road
London, SW7 2AZ, United kingdom
A.Giovannitti13@imperial.ac.uk

Dr. C.B. Nielsen
Materials Research Institute and School of Biological and Chemical Sciences,
Queen Mary University of London,
Mile End Road, London E1 4NS, United Kingdom

Dr. M.J. Donahue, Prof. G.G. Malliaras
Department of Bioelectronics
École Nationale Supérieure des Mines, CMP-EMSE, MOC
Gardanne, 13541, France

Prof. G.G. Malliaras
Electrical Engineering Division
University of Cambridge
9 JJ Thomson Ave, Cambridge CB3 0FA
United Kingdom

Prof. Jonathan Rivnay
Department of Biomedical Engineering,
Northwestern University, 2145 Sheridan Road,
Evanston, Illinois 60208-3109
and Simpson Querrey Institute,
Northwestern University, 303 E.
Superior, Suite 11-131, Chicago Illinois 60611, USA.

Prof. I. McCulloch
King Abdullah University of Science and Technology,
SPERC
Thuwal 23955-6900, Saudi Arabia.

Keywords: Organic bioelectronics, organic electrochemical transistors, organic semiconductors, quinones, stability

Abstract

Organic semiconductors can be employed as the active layer in accumulation mode organic electrochemical transistors (OECTs) where redox stability in aqueous electrolytes is important for long-term recordings of biological events. We observed that alkoxy-BDT copolymers can be extremely unstable when they are oxidised in aqueous solutions. The redox stability of these copolymers could be improved by molecular design of the copolymer where it was observed that the electron rich comonomer 3,3'-dimethoxy-2,2'-bithiophene lowers the oxidation potential and also stabilizes positive charges through delocalization and resonance effects. For copolymers where the comonomers do not have the same ability to stabilise positive charges, irreversible redox reactions were observed with the formation of quinone structures, being detrimental to performance of the materials in OECTs. Charge distribution along the copolymer from density functional theory calculations was seen to be an important factor in the stability of the charged copolymer. As a result of the stabilizing effect of the comonomer, a highly stable OECT performance was observed with transconductances in the mS range. The analysis of the decomposition pathway also raises questions about the general stability of the alkoxy-BDT unit, which is heavily used in donor-acceptor copolymers in the field of photovoltaics.

Introduction

Benzo[1,2-b:4,5-b′]dithiophene (BDT) structures with alkoxy chains in the 4,8-positions are a common building block for organic semiconductors due to their ability to form rigid backbone structures when copolymerized with thiophene-based comonomers. The planarity of the backbone is highly important to form ordered structures in the solid state, often a requirement for high charge carrier mobilities in organic semiconductors.[1–3] The alkoxy side chains in the 4,8-positions increase the electron density of the BDT structure compared to alkyl analogs due to overlap of the oxygen lone pairs and the aromatic system (resonance effect). The choice of the comonomer strongly affects the energy levels and electron distribution of the resulting copolymer which allows the preparation of alkoxy-BDT copolymers with various ionization

potentials (IPs), ranging from 4.4 eV to 5.2 eV[4–6] and allows the materials to be used in various applications such as organic photovoltaics (OPV)[7–9] and organic field effect transistors (OFETs).[10,11] Another advantage of the BDT monomer is the attachment of various side chains via simple alkylation reactions, contrary to other thiophene based units where side chains regularly need to be attached by metal activated coupling reactions.

The tunable highest occupied molecular orbital (HOMO) levels of easily oxidizable BDT-containing copolymers make them a promising candidate for future application in organic electrochemical transistors (OECTs), which have recently gained significant attention in the field of bioelectronics.[12,13] In contrast to other organic electronic devices which operate on the basis of charge carrier generation by either optical excitation (OPV) or accumulation of charges at an interface by applying an electric field (organic field-effect transistor (OFET)), OECTs operate on the basis of electrochemical doping of the active material through an electrolyte medium. Devices can be operated in accumulation[5,14,15] or depletion mode[16–19] where either a semiconducting or conducting material is used as the active material. Accumulation mode OECTs require a semiconductor exhibiting a low charge carrier density in its un-doped state, resulting in a low conductivity of the material. When the semiconductor is electrochemically oxidized, the charge carrier density, and thus the conductivity, increases. In addition, the increase of the conductivity strongly depends on the charge carrier mobility of the introduced charges where the microstructure of the organic semiconductor was found to be highly important.[5] Ideally, organic semiconductors for OECTs should exhibit a small ionization potential to allow for low turn on voltages of the device, as well as avoiding electrochemical side reactions with the bio-interface or the aqueous electrolyte which could degrade the materials.[20,21] While recent studies on the stability of organic semiconductors in OECTs showed a promising development towards stable operation,[14,21,22] a highly stable redox reaction of the semiconductor in aqueous electrolytes is still a challenge for organic materials.

BDT-containing copolymers have already received significant attention in the field of OPV[7] where the alkoxy-BDT thieno[3,4-b]thiophene copolymer PTB7,[9] with phenyl-C_{71}-butyric acid methyl ester ($PC_{71}BM$),[9] shows a power conversion efficiency (PCE) of up to 9.2%.[23] While the thiophene flanked BDT copolymers PTB7-Th[24] show an acceptable stability in OPV, many alkoxy-BDT copolymers decompose rapidly during operation and therefore cannot be used reliably in organic devices.[25,26]

A recent study showed that some alkoxy-BDT copolymers could be used to good effect in OECT devices, while others where inherently unstable under device operation.[5] In the current work we report on the factors determining the redox stability of alkoxy-BDT copolymers, and we find that the choice of the comonomer of alkoxy-BDT copolymers is important for their stability during electrochemical redox reactions in aqueous electrolytes. We observed that alkoxybithiophene units are able to stabilize positive charges on the polymer backbone which is important for long-term stability of the material during operation of OECTs. Previous reported alkoxy-BDT copolymers[5] and novel copolymers with large oxidation potentials are not able to stabilize positive charges on the polymer backbone and undergo an irreversible reaction forming quinone structures. The formation of quinones lowers the performance of the materials in OECTs significantly and make the materials impractical for operation in OECTs. Here, we reveal the decomposition pathway of the copolymers by spectroscopy and electrochemical measurements and show that molecular design of the copolymers is highly important for electrochemical redox stability. These results can be used as design guidelines for the alkoxy-BDT polymers and their application in the wider field of organic electronics encompassing OPV, OFET and OECT applications.

Results and Discussion

Polymer properties

The copolymers gBDT-TT, gBDT-T2[5] and gBDT-MeOT2 were prepared by Stille polymerization and the structures are shown in **Figure 1**. The comonomers were chosen to study the influence of the ionization potential on the electrochemical redox reactions in aqueous electrolytes as well as the performance in OECTs. The 3,3'-dimethoxy-2,2'-bithiophene (MeOT2) was selected because of its electron rich nature, and its planar structure due to non-covalent sulphur-oxygen interactions.[27] The thienothiophene unit (TT) was chosen as a planar unit being less electron rich than MeOT2. Finally, the non-planar bithiophene unit (T2) was selected as a comonomer to be similar in size with MeOT2 but electronically similar to the TT unit. The alkoxy-BDT monomer was substituted with polar triethylene glycol side chains to allow for facile ion penetration in the solid state when the polymers are oxidized in an aqueous electrolyte, making the polymers suited for OECTs.[5,14] Polymer gBDT-MeOT2 is soluble in $CHCl_3$ and TCE while gBDT-TT and gBDT-T2 are only soluble in TCE. The IPs were measured by cyclic voltammetry measurements in acetonitrile (Figure S13) and the results are summarized in Table 1. The gBDT-TT and gBDT-T2 copolymers have comparable ionization potentials (4.70 eV and 4.85 eV), while the IP decreases to 4.31 eV for gBDT-MeOT2 due to the more electron-rich MeOT2 comonomer. The optical band gap decreases from 2.1 eV for TT and T2, to 1.8 eV for MeOT2 (Figure S6). The molecular weight analysis for gBDT-TT and gBDT-T2 was inconclusive due to the low solubility of the polymers in common organic solvents for gel permeation chromatography (GPC) analysis (chloroform, DMF, chlorobenzene). The low molecular weight fraction of gBDT-MeOT2 was analyzed by mass spectrometry (MALDI-ToF) where up to 8 repeating units were detected (Figure S5). The higher molecular weight fraction of the polymers could not be characterized by mass spectrometry.

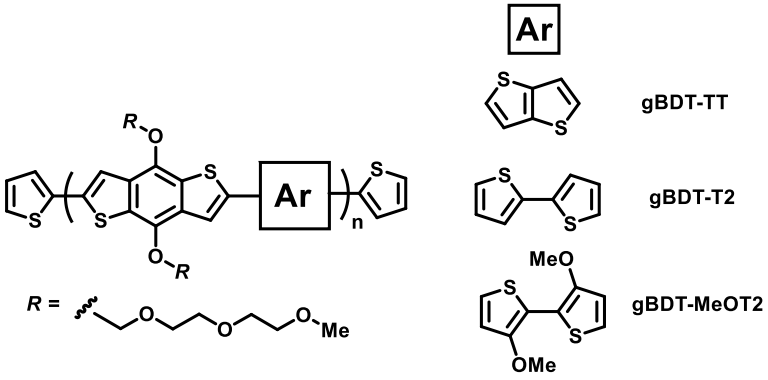

Figure 1. Chemical structures of BDT polymers gBDT-TT, gBDT-T2 and gBDT-MeOT2.

Density functional theory (DFT) calculations were carried out to analyze the geometries of the polymer backbones as well as the highest occupied molecular orbital (HOMO) energy levels. Through torsional angle analysis (B3LYP-D3/6-31G*), the MeOT2 unit was found to favor a coplanar geometry with a barrier of rotation of 4 kcal/mol (Figure S20) between the two thiophenes, as observed for similar alkoxybithiophene analogues.[27,28] All other thiophene-thiophene rotations were found to have potential minima at dihedral angles of +/- 160° between sulfur atoms, with a small barrier of rotation of 0.1 kcal/mol between them. Other local minima, destabilized by 1.5 kcal/mol relative to the global minimum, were found at +/- 50°. The findings suggest that gBDT-TT and gBDT-MeOT2 possess similarly twisted backbones in the gas phase, while the backbone twist is further increased in gBDT-T2 based on the additional twist of the bithiophene unit (Figure S20). The calculated energy levels for the three polymers, modelled as five repeating BDT-Ar units, using IP-tuned functionals (ωB97XD/6-31G*) are presented in Table 1. The energy of the HOMO in vacuum of the T2 and TT containing polymers have similar energies of -6.3 eV and -6.2 eV, respectively, while the HOMO of the gBDT-MeOT2 structure increased to -5.6 eV. The trend in energies is consistent with values obtained from cyclic voltammetry (CV).

Table 1 Properties of the alkoxy-BDT copolymers

Polymer	IP [a] [eV]	Oxidation onset [b] [V]	Optical band gap [eV]	Absorption onset [nm]	Calculated HOMO energy [eV] [c]
gBDT-T2	4.85	0.6 V	2.1	600	-6.3
gBDT-TT	4.70	0.5 V	2.1	588	-6.2
gBDT-MeOT2	4.31	-0.2 V	1.8	679	-5.6

a) CV measurements on indium tin oxide (ITO) glass substrates with a 0.1 M NBu_4PF_6 in acetonitrile (Figure S13)
b) CV Oxidation onset of the polymers on ITO coated glass substrates, measured in aqueous solution vs Ag/AgCl (Figure 2a)
c) Gas-phase HOMO energies calculated using IP-tuned ωB97XD/6-31G* for polymer fragments with five repeating BDT-Ar units.

The CV measurements of polymer thin films coated on indium tin oxide (ITO) coated glass substrates in aqueous solutions were carried out to measure the oxidation potentials and stability of redox reactions. As shown in **Figure 2a**, the oxidation onset of gBDT-TT and gBDT-T2 is 0.45 V and 0.50 V vs Ag/AgCl, respectively, while the substitution of the comonomer to the electron rich MeOT2 unit shifts the oxidation onset to -0.20 V. Spectroelectrochemical measurements were carried out to get further insight into the charging process of the polymer. Figure 2b presents the evolution of the thin film absorption spectrum of gBDT-MeOT2 when a voltage of -0.2 to 0.7 V vs Ag/AgCl is applied. The intensity of the main absorption peak (S0-S1) decreases successively when the potential is gradually increased. Simultaneously, a new absorption peak appears at longer wavelength between 700 and 1100 nm with an isosbestic point at 660 nm. The decrease in intensity of the S0-S1 transition can be explained by the depletion of electrons from the HOMO level. A higher lying singly occupied molecular orbital (SOMO) forms, where the polaron absorption can be observed at lower energies as previously reported in the literature.[5,14,29,30] The charging of the polymer is highly reversible at potentials up to 0.7 V where high doping states are achieved and the initial absorption spectrum can be restored by applying a voltage of -0.3 V as shown in Figure S19. At potentials between 0.7 V and 1V, bipolaron formation is observed, as demonstrated by the

increasing absorption at 1100nm and a new isosbestic point at 900 nm (Figure S14b,c), similar to electrochemical oxidation of P3HT.[31] Beyond 1 V, the absorption of both the polaron and bipolaron drop in intensity as a new peak is formed at 385 nm with an approximate isosbestic point at 445 nm. This represents an irreversible oxidation process as the initial neutral polymer absorption cannot be fully recovered when the potential is reversed to -0.3V. A different observation was obtained for the polymers with a larger IP. Figure 2c shows the spectroelectrochemical measurements of gBDT-TT where the S0-S1 absorption peak first decreases when applying a voltage, and an absorption peak for the polaron can be observed at longer wavelength, similar to gBDT-MeOT2. However, at voltages higher than 0.6 V, no further decrease of the S0-S1 peak is observed, while the intensity of the polaron absorption peak decreases and a new absorption feature around 400 nm emerges, which is discussed in more detail below. The oxidation of the polymer is extremely unstable and it is not possible to restore the initial absorption spectrum by reversing the potential (Figure S17). Similar results were obtained for measurements of gBDT-T2 (Figure S18).

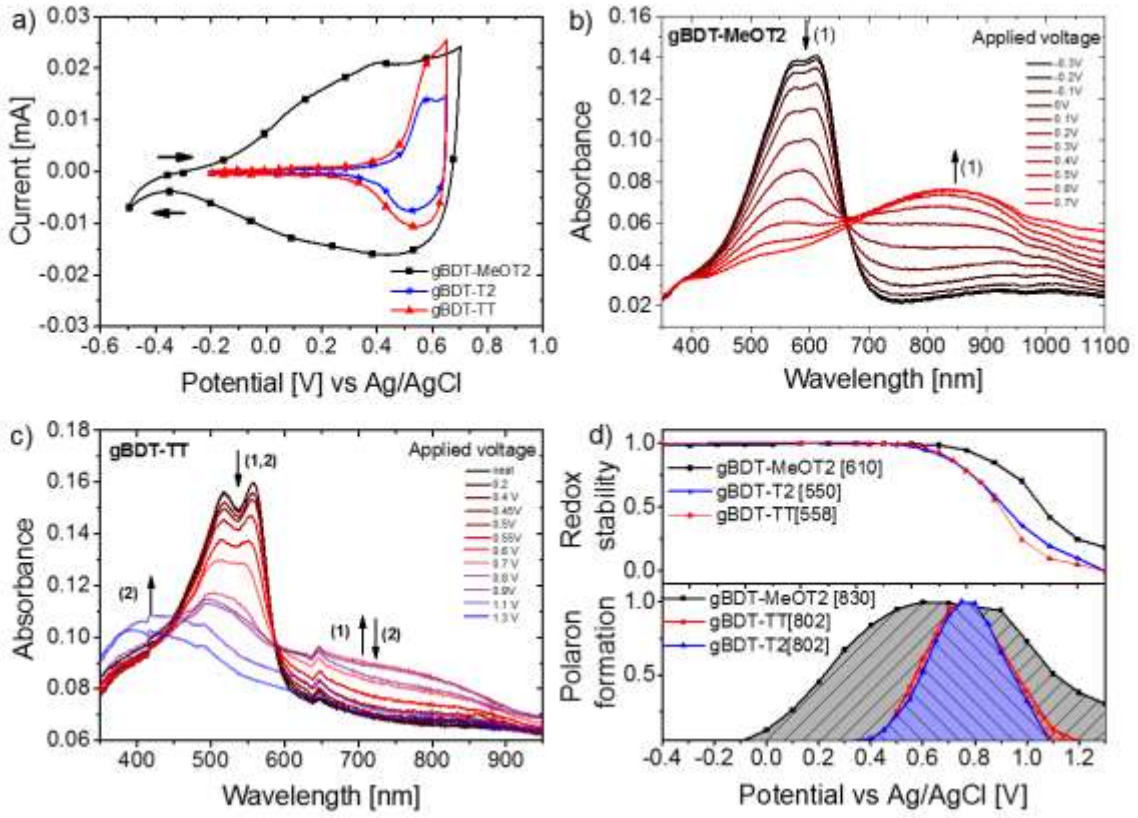

Figure 2. Electrochemical oxidation and changes in absorption. (a) Cyclic voltammetry of polymer thin films with a scan rate of 100mV/s, (b) spectroelectrochemical measurements of gBDT-MeOT2, (c) spectroelectrochemical measurements of gBDT-TT ((1) formation of polaron, (2) decomposition) and (d) comparison of the redox stability of the polymers after applying the indicated voltages and reversing the voltage to reduce the copolymer (top, redox stability of the copolymers (at the indicated wavelength) showing the difference of absorbance of the pristine copolymer (at -0.3 V) and oxidized copolymer (indicated voltage, then reversing the voltage to -0.3 V, normalized to the maximum value) and formation of the polaron at the indicated wavelengths (bottom, normalized polaron absorbance (λ_{max}(polaron)) at the indicated wavelength, area underneath the curves are highlighted, note that the area underneath the curves does not represent the amount of introduced charges). The measurements were carried out in degassed 0.1 M NaCl aqueous solution.

The stabilities of the three polymers were studied by applying a voltage for 60 seconds, and then remeasuring the absorption spectra at a reversed voltage (-0.3 or 0V). The loss in absorptivity directly relates to how much polymer has been degraded by the initial applied voltage (Figure 2d). The polaron absorption is also plotted versus the applied potential. Polymer gBDT-MeOT2 forms a polaron at low voltages where the polymer is redox stable. The initial small decrease in polaron absorption at 0.7 V is due to bipolaron formation, and decomposition is only observed after this point. The TT and T2 polymers form polarons at

higher voltages than gBDT-MeOT2, which quickly decompose to form the blue-shifted species. The changes of the polymers' absorption spectra after applying a voltage offset is summarized in Figures S17-19. The trends discussed here mirror existing evidence that while low HOMO polymers are more stable toward oxygen and water in the neutral state, the electrochemically oxidized polymer follows the opposite trend, and that a higher lying HOMO leads to greater stability.[32] The comparatively low HOMO levels / large IP energies of gBDT-T2 and gBDT-TT/T2 lead to highly oxidizing polarons that result in polymer degradation.

Polymer decomposition pathway

Given the differences in stability of the three polymers observed by electrochemical studies, we further investigated the decomposition reaction of the BDT-containing polymers. The alkoxy-BDT unit can potentially be oxidized at the 4,8-positions to form a quinone structure. This transformation is possible by chemical oxidation with strong oxidants such as cerium ammonium nitrate (CAN).[33] For the conjugated polymers in this study, we identified two possible outcomes which can occur during the electrochemical oxidation. Either an electron can be removed and the positive charge (polaron/radical cation) can be stabilized on the polymer backbone, or an irreversible side reaction can occur which forms the quinone structure with loss of the alkoxy side chains. The formation of the quinone structure would have a strong effect on the polymer performance in electronic devices. Specifically, it would result in a decrease of the donor strength, as well as breaking the effective conjugation by the introduction of electron withdrawing quinone groups. Both cases directly influence the ionization potential, absorption profile, and charge carrier transport.

Spectroscopic evidence suggests quinone formation for the gBDT-TT and gBDT-T2 polymers and a stable p-type doping redox reaction for gBDT-MeOT2 up to 0.7 V, at which the polymer is highly doped. For the TT and T2 polymers, the absorption spectrum of the polymer blue-shifts and broadens in the visible region after electrochemical oxidation as shown in Figure 2c

and Figure S18 which is in agreement with previous studies on the degradation of BDT containing polymers.[25,34] A color change of the polymers is observed from red to yellow/brown (Figure S23 and S24). The shift towards shorter wavelength and the decrease of the neutral polymer and polaron absorption peaks of the gBDT polymers are consistent with irreversible oxidation of the BDT units at various points along the polymer resulting in shorter conjugated segments of varying lengths. Since the polymer becomes insoluble in organic solvents after the electrochemical reactions, infrared (IR) spectroscopy proved to be the technique of choice to analyze the decomposition product. Compared to the pristine materials, a new absorption peak at 1656 cm^{-1} for the gBDT-Br_2 monomer, 1653 cm^{-1} for gBDT-TT and 1654 cm^{-1} for gBDT-T2 is observed after electrochemical oxidations as shown in **Figure 3 (a-c)**. In contrast, neither the formation of an insoluble film, nor the appearance of an IR-peak around 1650 cm^{-1} was observed for gBDT-MeOT2 (Figure 3d) when applying up to 0.7 V.

To verify the origin of the new IR peak, the spectrum of a 4,8-dialkoxy-BDT monomer was compared to that of benzo[1,2-b:4,5-b′]dithiophene-4,8-dione (Figure S32) and literature data for poly(benzo[1,2-b:4,5-b′]dithiophene-4,8-dione-2,6-diyl),[35] where the carbonyl stretches of the quinone structure can be found at 1639 cm^{-1} and 1652 cm^{-1}, respectively. These findings suggest that the new signals observed after oxidation of the large IP polymers at similar wavenumbers around 1650 cm^{-1} can be assigned to be the quinone C=O bond stretch. In contrast to other studies of BDT containing polymers such as PTB7, the polymers presented here do not include additional carbonyl groups as side chains of the polymer, allowing us to identify the newly formed quinone functionality through IR spectroscopy. In comparison, several oxidation cycles of gBDT-MeOT2 showed no formation of the C=O stretch peak at voltages up to 0.7 V which indicates that the polymer is able to stabilize the positive charge (polaron) during electrochemical oxidation reactions. The polymer starts to decompose when a bipolaron is formed as shown in Figure S25. Further analysis of the chemical oxidation

product of the alkoxy-BDT monomer by mass spectrometry and ^{1}H NMR spectroscopy support the presented decomposition pathway of the BDT unit, where both the quinone structure and triethylene glycol side chain were identified to be the decomposition products (Figure S30-S31).

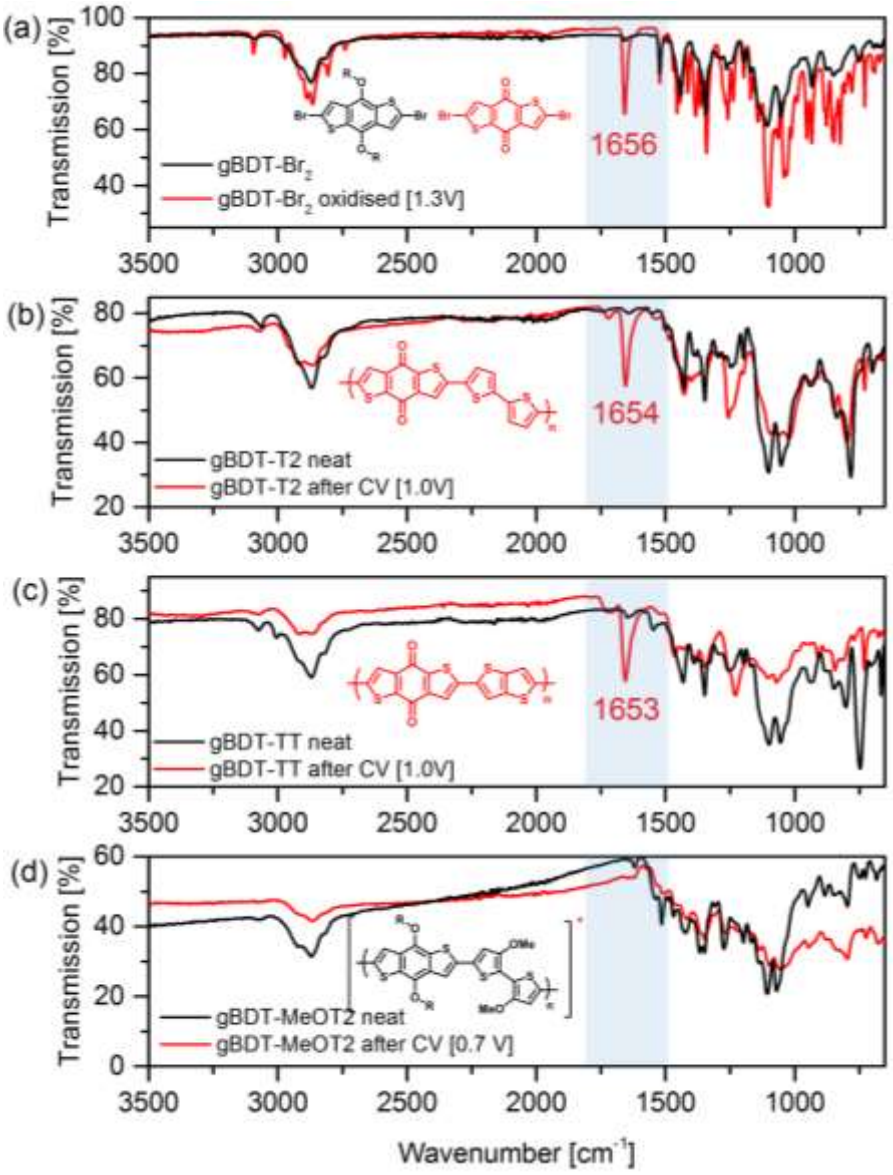

Figure 3. IR spectra and analysis of the decomposition products. (a) Quinone formation of the monomer BDT-Br_2 after applying 1.3 V (Figure S27), (b, c) quinone formation of the polymers gBDT-TT and gBDT-T2 after applying 1.0 V and (d) stable redox-reaction for gBDT-MeOT2 and no evidence of quinone formation after applying 0.7 V (polaron formation). The corresponding CV measurements are presented in Figures S23-S25. Quinone formation of gBDT-MeOT2 can be observed after applying up to 1.5 V (Figure S26).

Our suggestion for the decomposition mechanism is most likely activated by the oxidation of the alkoxy-BDT copolymers and formation of the radical cation (polaron) as shown in Figure S28. A water molecule can attack the positive charged polymer to form a tetrahedral intermediate on the carbon adjacent to the ether oxygen. Then, the triethylene glycol side chain leaves the molecule under formation of a ketone. The same reaction could occur on the other side to form the quinone. Cycloaddition of an oxygen molecule could lead to the same quinone product, but since degassed electrolyte were used, we believe that water is the most likely source of oxygen.

The proposed decomposition products of polymers gBDT-T2 and gBDT-TT (i.e. the poly(dithiophene-4,8-dione-2,6-diyl)-bithiophene and -thienothiophene polymers) may be able to be reduced to form the sodium alkoxide structure[35] as illustrated in **Figure 4a**. Cyclic voltammetry measurements were carried out before and after the oxidation of the polymers (Figure 4b,c). Initially, no reduction peak is observed but after applying a potential above 0.7 V, further cycles exhibited reversible reduction peaks at potentials of -0.42 V (TT) and -0.48 V (T2), supporting the formation of the quinone containing polymer. In contrast, gBDT-MeOT2 is stable up to 0.7 V and does not show any indication of the reduction peak during further cycling. CV measurements were also carried out for the BDT-Br_2 monomer (Figure S27), where no reduction peak was observed during the first cycle. Only after oxidizing the monomer at 0.9 V, a distinctive reduction peak could be observed, indicating the formation of the quinone structure.

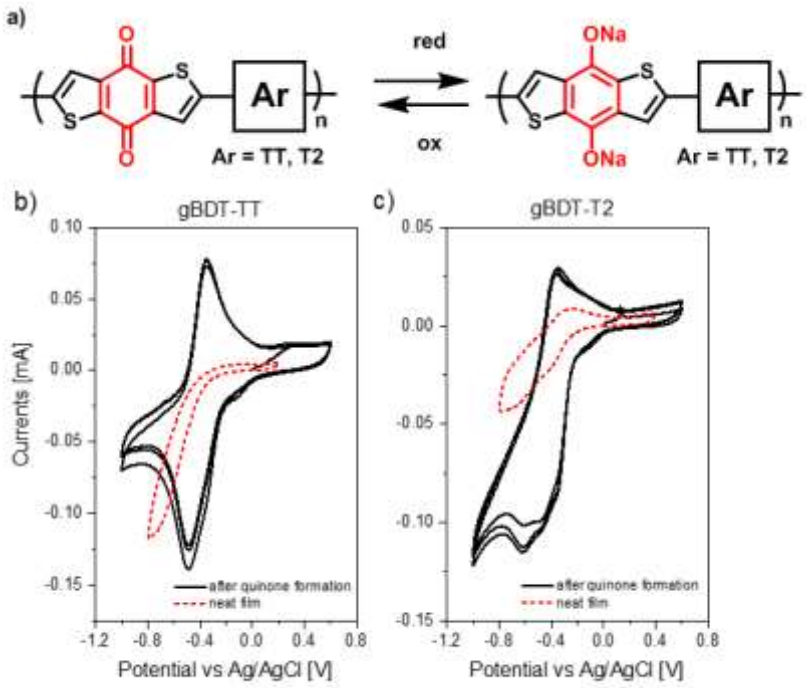

Figure 4. (a) Reduction of the quinone containing copolymers to form the sodium alkoxide structure and (b) CV measurements before (red dashed line) and after oxidation (black line) of the large IP polymers with degassed 0.1 M NaCl aqueous solution.

Several stability studies on PTB7 and polymer analogues have been reported where the addition of hydroxyl groups on the BDT unit[25] or the oxidation of the polymer by cycloaddition of oxygen,[34] quinone formation[36] or singlet oxygen generation from triplet excitons[26] were suggested decomposition products. Our findings are in agreement with irreversible polymer oxidation. Quinone formation was already suggested as the product upon irradiation of BDT monomers with UV light for several minutes, based on changes in the ^{1}H nuclear magnetic resonance (NMR) spectrum.[36] In addition, Alem and coworkers observed a blue shift in the absorption spectrum and incomplete recovery of absorption intensity after photo degradation, similar to that observed for the oxidized polymers gBDT-TT and gBDT-T2.[34] In their publication, they report the cleavage of the side chain which was confirmed by ^{1}H NMR spectroscopy. The findings are in agreement with our observations where the alkoxy-BDT monomer was chemically oxidized and a cleavage of the side chain was observed (Figure S29). With these considerations in mind, we believe that the irreversible quinone formation

evidenced herein is likely to be a dominant degradation mechanism not only for the gBDT copolymers presented here, but also for the numerous other BDT copolymers used in organic electronic applications.

While the changes in HOMO energy levels can be used to explain the trend in polaron stability as previously reported[32], further insight comes from DFT calculations. Population analysis of the HOMO of the neutral polymer and the equivalent unoccupied orbital in the radical cation form were carried out to quantify the orbital density distribution along the polymer chain (**Figure 5** and S22). Atoms of the polymer repeating units were assigned to either BDT or comonomer (Ar) fragments so that the contribution of the different units could be easily identified. As the electron donating ability of the comonomer was increased, the HOMO and singly unoccupied molecular orbital (SUMO) become increasingly localized on the comonomers rather than BDT unit. Summation of the fragment orbital distributions of the repeating units leads to the total orbital distribution in gBDT-TT (60% BDT, 40% TT) switching completely around in gBDT-MeOT2 (20% BDT, 80% MeOT2). The same trend is also observed with the Mulliken charge analysis in the positively charged polymer. Although there is an increase in the size of the comonomer when going from TT to MeOT2 which will certainly contribute to the change in percentage of orbital density, the bithiophene linker T2 serves as a good point of reference, being comparable in size to MeOT2 and similar in energy to TT. It appears that the key factor for the polaron stabilization is the electron donating character of the MeOT2 comonomer which can stabilize the positive charge and prevent a high charge density on the BDT unit. In addition, a lower localization of the wave function on the C-O bond of the alkoxy-BDT unit is also observed. Therefore, the more electron rich polymer gBDT-MeOT2 tends to be the most stable polymer for electrochemical oxidation compared to the more electron deficient ones which tend to form the quinone by-product during electrochemical oxidation.

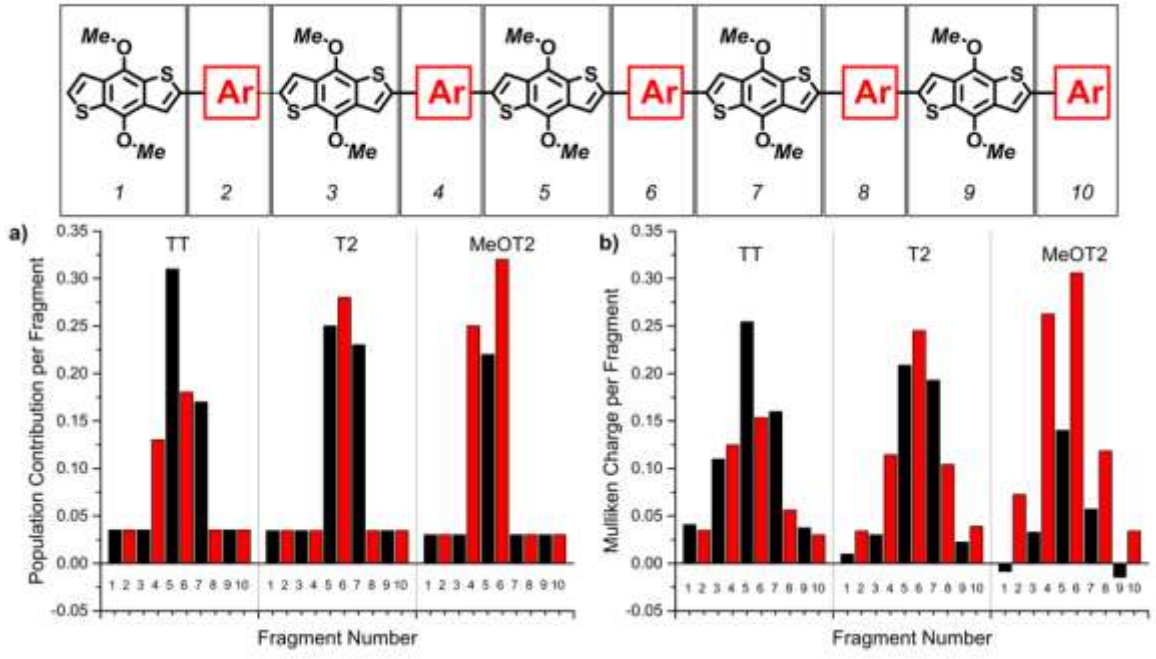

Figure 5. DFT calculations. (a) Singly unoccupied molecular orbital (SUMO) and (b) charge distribution in polymers gBDT-TT, gBDT-T2 and gBDT-MeOT2 bearing a positive charge, calculated at tuned-ωB97XD/6-31G*. Each vertical bar represents the contribution from different fragments along the polymer chain (BDT in black, thiophene comonomer in red).

OECT devices

To validate the relevance of these stability concepts in devices, the polymers were tested as the active material in p-type accumulation mode OECTs where a reversible electrochemical redox-reaction is required to increase the charge carrier density and hence the conductivity of the active layer. Since gBDT-MeOT2 has the lowest oxidation potential, it should exhibit the lowest turn on voltage of the polymer series. The output and transfer curves of gBDT-MeOT2 based OECTs are shown in **Figure 6(a,b)**, where a turn on voltage of -0.05 V was observed. The performance of the materials can be evaluated by the transconductance ($g_m = \partial I_d/\partial V_g$), a measure for how effectively the current is modulated when varying the gate voltage. The OECT performance of the polymer series is summarized in Table 2 where the normalized gBDT-MeOT2 affords the highest performance of alkoxy-BDT type polymers so far tested in OECTs.[5] Since the transconductance scales with Wd/L of the active channel (with W, width; d, thickness, and L, channel length),[19] similar channel dimensions and thicknesses of the

active layer were chosen to compare the performance (Figure S10). In contrast, gBDT-TT and gBDT-T2 have a lower transconductance by almost two orders of magnitude, mostly due to the low doping state of the polymers before the polymers degrade. Electrical impedance spectroscopy (EIS) was carried out to extract the volumetric capacitance [F/cm³] when a voltage offset is applied. For gBDT-MeOT2, a volumetric capacitance of 95 F/cm³ at V_g = 0.6 V was measured (Figure S12) which is more than twofold the value reported for PEDOT:PSS[19], most likely due to the absence of an electrically insulating polyelectrolyte. The polymers gBDT-TT and gBDT-T2 could not be analyzed by EIS measurements due to instability during the oxidation of the polymers.

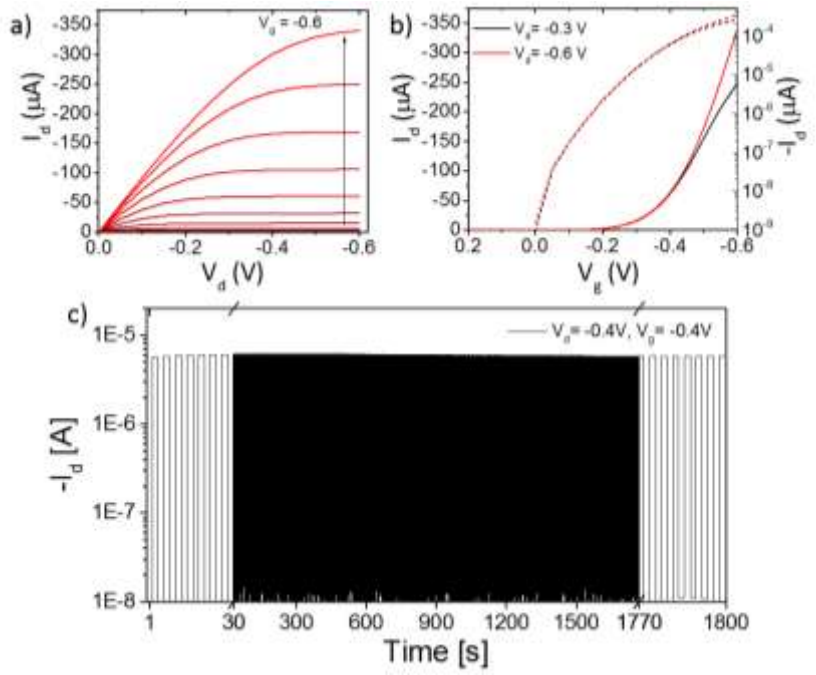

Figure 6. OECT performance of gBDT-MeOT2 with (a) output curve for −0.6 V < V_g < 0 V (ΔV_g = 0.05 V), (b) transfer curve at V_d = -0.3 V and -0.6 V for device dimensions of W = 100 µm, L = 10 µm and d = 124 nm and (c) stability measurement of the OECT for 30 min with V_d = -0.4 V and applying voltage pulses between V_g = 0 V and -0.4 V (the beginning and end of the pulse experiment is highlighted (30 seconds).

Table 2: OECT performance of the polymers with [W = 100 µm, L = 10 µm].

	T2	TT	MeOT2
g_m [mS] (at V_g[V])	0.06 (0.65)	0.09 (0.65)	1.82 (0.6)
d [nm]	102	80	125
Norm.g_m [S/m][b)]	59	113	1460
V_{ON} [V]	-0.6	-0.55	-0.1
ON/OFF ratio	$1.0*10^4$	$5.2*10^3$	$4.9*10^6$
C*[F/cm³]	-[a)]	-[a)]	95

a) The capacitance could not be analyzed due to decomposition of the polymers when applying a voltage offset.
b) Transconductance was normalized by Wd/L with W = 100 µm, L = 10 µm and the indicated thickness d.

The device with gBDT-MeOT2 as the active material demonstrate stable operation during pulse experiments for 30 min. This is shown in Figure 6c where the ON-currents decreased by only 7 % after 300 pulses, exhibiting a stability comparable to state of the art accumulation mode p-type polymers.[14] The polymers gBDT-TT and gBDT-T2 show a higher turn on voltage of -0.55 V and -0.60 V, which is in agreement with the observed oxidation potentials measured by CV. When the gate voltage is then stepwise increased to allow for a higher degree of doping of the polymers, a significant decrease of the drain currents can be observed, most likely due to the formation of the quinone structure, making the polymers impractical for long term operation (Figure S11). These findings suggest that when alkoxy-BDT based copolymers are the choice of materials, an electron rich comonomer is needed which has to be able to stabilize the positive charges on the polymer backbone and therefore allow for a stable operation in OECTs.

Conclusions

We have demonstrated the ability to increase the stability of alkoxy-BDT copolymers and their applications in accumulation mode organic electrochemical transistors (OECTs). A previous study has reported on the performance of alkoxy-BDT copolymers in OECTs but didn't venture far into the issues regarding stability.[5] Here, we describe the redox-stability in aqueous

electrolytes and observed a strong dependency of stability and choice of the comonomer unit. The decomposition product for the less stable polymers could be identified as a quinone structure which interrupts the charge transport and changes the optoelectronic properties of the polymers. Copolymers with the electron rich and coplanar comonomer 3,3'-dimethoxy-2,2'-bithiophene exhibited the highest stability during electrochemical oxidation and are able to stabilize a polaron on the polymer backbone due to the increased charge stabilization of the methoxybithiophene unit as well as a reduced orbital and charge density on the BDT groups. The increased stability for thin films of polymer gBDT-MeOT2 during electrochemical oxidation in aqueous solution was confirmed by showing a highly stable OECT in aqueous environments.

These findings suggest that for the design of future copolymers based on the alkoxy-BDT repeating unit, the choice of the comonomer is essential to allow the preparation of conjugated polymers which can be employed in organic electronic devices where the polymer needs to be able to stabilize electronic charge carriers. This might be achieved by assessing the redox properties of the isolated comonomer through computation or electrochemical measurements before synthesizing the polymer. In a broader context, our findings highlight that molecular design of semiconducting copolymers can be further advanced by careful consideration of the electronic interplay between the chosen comonomers. Additionally, apparent instabilities of important monomer building blocks can be alleviated by careful choice of the comonomer.

Experimental section

Synthesis

(3,3'-dimethoxy-[2,2'-bithiophene]-5,5'-diyl)bis(trimethylstannane): A 150 mL two neck RBF was dried and purged with argon. 3,3'-dimethoxy-2,2'-bithiophene (1.13 g, 5.0 mmol) was dissolved in 60 mL of anhydrous THF. At -78 °C, *n*-BuLi (2.5 M in THF) (8.0 mL, 20.0 mmol) was added dropwise with stirring and the reaction mixture was allowed to heat up to room temperature. The reaction mixture was cooled to -78 °C again and Me_3SnCl (1.0 M solution in THF) (20 mL, 20.0 mmol) was added, followed by heating the reaction mixture to room temperature. The reaction mixture was diluted with water followed by the addition of 100 mL of diethyl ether. The organic layer was washed with water (3 x 50 mL), dried over Na_2SO_4 and the solvent was removed *in vacuo*. The crude product was recrystallized from acetonitrile to afford the target molecule as white crystals with a yield of 73 % (2.01 g, 3.65 mmol). ^{1}H NMR (400 MHz, acetonitilre-d_4, δ): 7.04 (s, 2H), 3.92 (s, 6H), 0.37 (s, 18H). ^{13}C NMR (100 MHz, $CDCl_3$, δ): 156.4, 136.3, 125.3, 120.5, 59.83. HRMS (ES-ToF): 552.9479 $[M+H]^+$ (calc. 552. 9491 $C_{16}H_{27}O_2S_2Sn_2$).

gBDT-T2 was synthesized according to a literature procedure.[5]

gBDT-TT: In a 2.0 mL microwave vial 2,6-dibromo-4,8-bis(2-(2-(2-methoxyethoxy)ethoxy)-ethoxy)benzo[1,2-b:4,5-b']dithiophene (83.32 mg, 0.124 mmol) and 2,5-bis(trimethylstannyl)-thieno[3,2-b]thiophene (57.72 mg, 0.124 mmol) were dissolved in 1.0 mL of anhydrous, degassed chlorobenzene. $Pd_2(dba)_3$ (2.27 mg, 2.5 µmol) and P(*o*-tol)$_3$ (3.05 mg , 9.9 µmol) were added and the reaction mixture was purged with argon for 5 min. The vial was transferred to a microwave and heated to 100 °C for 5 min, 120 °C for 5 min, 140 °C for 5 min, 160 °C for 5 min, 180 °C for 5 min, 200 °C for 25 min. The end-capping procedure was carried out according to the protocol described in the Supporting Information (SI). A red solid was obtained which was washed with methanol and transferred into a Soxhlet thimble. Soxhlet extraction was carried out with methanol, hexane, acetone, tetrahydrofuran and chloroform. The remaining polymer was isolated and dried under high vacuum for 16 h. 30 mg (0.046 mmol) of the polymer was obtained with a yield of 37 % (this fraction of the polymer is soluble in 1,1,2,2-tetrachloroethane (TCE)). ^{1}H NMR (400 MHz, TCE-d_2, δ):7.43-6.81 (m, 4H), 4.61-4.17 (m, 4H), 4.17-3.48 (m, 20H), 3.39 (broad s, 6 H) ppm.

gBDT-MeOT2: In a 2.0 mL microwave vial 2,6-dibromo-4,8-bis(2-(2-(2-methoxyethoxy)ethoxy)-ethoxy)benzo[1,2-b:4,5-b']dithiophene (63.64 mg, 94.5 µmol) and (3,3'-dimethoxy-[2,2'-bithiophene]-5,5'-diyl)bis(trimethylstannane) (52.23 mg, 94.5 µmol) were dissolved in 2.0 mL of anhydrous, degassed chlorobenzene. $Pd_2(dba)_3$ (1.73 mg, 1.89 µmol) and P(*o*-tol)$_3$ (2.30 mg, 7.56 µmol) were added and the reaction mixture was purged with argon for 5 min. The vial was transferred to a heating block and heated to 135 °C for 16 h. The end-capping procedure was carried out according to the end-capping protocol described in the SI. A purple solution was obtained which was precipitated in ethyl acetate and the precipitate was transferred to a Soxhlet thimble. Soxhlet extraction was carried out with ethyl acetate, methanol, hexane, acetone and chloroform where 7 mg (0.009 mmol) of the polymer was isolated from the chloroform fraction (10% yield). The remaining polymer was isolated and dried under high vacuum for 16 h. Additional 24 mg (0.033 mmol) of the polymer was obtained with a yield of 34 % (this fraction of the polymer is soluble in TCE). ^{1}H NMR (400 MHz, $CDCl_3$, δ): 4.62-4.38 (m, 4H), 4.24-4.06 (m, 4H), 3.93-3.80 (m, 4H), 3.80-3.70 (m, 12H), 3.51 (broad s, 6H), 3.31 (broad s, 6H) ppm.

Calculations

DFT calculations were carried out using Gaussian09.[37] Analysis of molecular energies as a function of torsional angle between aromatic groups was performed on fragments of the polymer to identify starting angles close to global minima, using B3LYP-D3/ 6-31G*. Optimized geometries and frequency analyses of polymer fragments with between 2 and 5 repeating units (BDT plus Ar group) were obtained at the ωB97XD/6-31G* level. The range separation parameter, ω, was then tuned to minimize the difference between the HOMO energy and the ionization potential, with further single point energy calculations using this tuned functional.

Device Fabrication

OECTs were fabricated as previously reported[5,16] spin casting the polymer gBDT-TT and gBDT-T2 from TCE. The low molecular weight fraction of gBDT-MeOT2 was dissolved in chloroform ($CHCl_3$) and either spin cast or drop cast.

Supporting Information

Supporting Information is available from the Wiley Online Library or from the author.

Acknowledgements

The authors thank KAUST, BASF, EPSRC Project EP/G037515/1, EP/M005143/1, EP/N509486/1, EC FP7 Project SC2 (610115), and EC H2020 Project SOLEDLIGHT (643791) for the financial support.

References

[1] S. Holliday, J. E. Donaghey, I. McCulloch, *Chem. Mater.* **2014**, *26*, 647.

[2] H. Pan, Y. Li, Y. Wu, P. Liu, B. S. Ong, S. Zhu, G. Xu, *Chem. Mater.* **2006**, *18*, 3237.

[3] Y. Tsutsui, G. Schweicher, B. Chattopadhyay, T. Sakurai, J.-B. Arlin, C. Ruzié, A. Aliev, A. Ciesielski, S. Colella, A. R. Kennedy, V. Lemaur, Y. Olivier, R. Hadji, L. Sanguinet, F. Castet, S. Osella, D. Dudenko, D. Beljonne, J. Cornil, P. Samorì, S. Seki, Y. H. Geerts, *Adv. Mater.* **2016**, *28*, 7106.

[4] J. Hou, M.-H. Park, S. Zhang, Y. Yao, L.-M. Chen, J.-H. Li, Y. Yang, *Macromolecules* **2008**, *41*, 6012.

[5] C. B. Nielsen, A. Giovannitti, D.-T. Sbircea, E. Bandiello, M. R. Niazi, D. A. Hanifi, M. Sessolo, A. Amassian, G. G. Malliaras, J. Rivnay, I. McCulloch, *J. Am. Chem. Soc.* **2016**, *138*, 10252.

[6] M. Heeney, C. Bailey, S. Tierney, W. Zhang, I. McCulloch, US Patent 7524922, **2005**.

[7] H. Yao, L. Ye, H. Zhang, S. Li, S. Zhang, J. Hou, *Chem. Rev.* **2016**, *116*, 7397.

[8] J. Hou, M.-H. Park, S. Zhang, Y. Yao, L.-M. Chen, J.-H. Li, Y. Yang, *Macromolecules* **2008**, *41*, 6012.

[9] Y. Liang, Z. Xu, J. Xia, S.-T. Tsai, Y. Wu, G. Li, C. Ray, L. Yu, *Adv. Mater.* **2010**, *22*, E135.

[10] C. Lu, H.-C. Chen, W.-T. Chuang, Y.-H. Hsu, W.-C. Chen, P.-T. Chou, *Chem. Mater.* **2015**, *27*, 6837.

[11] H. Pan, Y. Li, Y. Wu, P. Liu, B. S. Ong, S. Zhu, G. Xu, *J. Am. Chem. Soc.* **2007**, *129*, 4112.

[12] J. Rivnay, R. M. Owens, G. G. Malliaras, *Chem. Mater.* **2014**, *26*, 679.

[13] T. Someya, Z. Bao, G. G. Malliaras, *Nature* **2016**, *540*, 379.

[14] A. Giovannitti, D.-T. Sbircea, S. Inal, C. B. Nielsen, E. Bandiello, D. A. Hanifi, M. Sessolo, G. G. Malliaras, I. McCulloch, J. Rivnay, *Proc. Natl. Acad. Sci.* **2016**, *113*, 12017.

[15] S. Inal, J. Rivnay, P. Leleux, M. Ferro, M. Ramuz, J. C. Brendel, M. M. Schmidt, M. Thelakkat, G. G. Malliaras, *Adv. Mater.* **2014**, *26*, 7450.

[16] D. Khodagholy, J. Rivnay, M. Sessolo, M. Gurfinkel, P. Leleux, L. H. Jimison, E. Stavrinidou, T. Herve, S. Sanaur, R. M. Owens, G. G. Malliaras, *Nat. Commun.* **2013**, *4*, 2133.

[17] D. Khodagholy, T. Doublet, P. Quilichini, M. Gurfinkel, P. Leleux, A. Ghestem, E. Ismailova, T. Hervé, S. Sanaur, C. Bernard, G. G. Malliaras, *Nat. Commun.* **2013**, *4*, 1575.

[18] J. Rivnay, P. Leleux, M. Sessolo, D. Khodagholy, T. Hervé, M. Fiocchi, G. G. Malliaras, *Adv. Mater.* **2013**, *25*, 7010.

[19] J. Rivnay, P. Leleux, M. Ferro, M. Sessolo, A. Williamson, D. A. Koutsouras, D. Khodagholy, M. Ramuz, X. Strakosas, R. M. Owens, C. Benar, J.-M. Badier, C. Bernard, G. G. Malliaras, *Sci. Adv.* **2015**, *1*.

[20] D. M. de Leeuw, M. M. J. Simenon, A. R. Brown, R. E. F. Einerhand, *Synth. Met.* **1997**, *87*, 53.

[21] A. Giovannitti, C. B. Nielsen, D.-T. Sbircea, S. Inal, M. Donahue, M. R. Niazi, D. A. Hanifi, A. Amassian, G. G. Malliaras, J. Rivnay, I. McCulloch, *Nat. Commun.* **2016**, *7*, 13955.

[22] E. Zeglio, M. M. Schmidt, M. Thelakkat, R. Gabrielsson, N. Solin, O. Inganäs, *Chem. Mater.* **2017**, *29*, 4293.

[23] Z. He, C. Zhong, S. Su, M. Xu, H. Wu, Y. Cao, *Nat Phot.* **2012**, *6*, 591.

[24] Z. He, B. Xiao, F. Liu, H. Wu, Y. Yang, S. Xiao, C. Wang, T. P. Russell, Y. Cao, *Nat Phot.* **2015**, *9*, 174.

[25] J. Razzell-Hollis, J. Wade, W. C. Tsoi, Y. Soon, J. Durrant, J.-S. Kim, *J. Mater. Chem. A* **2014**, *2*, 20189.

[26] Y. W. Soon, H. Cho, J. Low, H. Bronstein, I. McCulloch, J. R. Durrant, *Chem. Commun.* **2013**, *49*, 1291.

[27] A. Giovannitti, C. B. Nielsen, J. Rivnay, M. Kirkus, D. J. Harkin, A. J. P. White, H. Sirringhaus, G. G. Malliaras, I. McCulloch, *Adv. Funct. Mater.* **2016**, *26*, 514.

[28] J. Huang, Y. Tang, K. Gao, F. Liu, H. Guo, T. P. Russell, T. Yang, Y. Liang, X. Cheng, X. Guo, *Macromolecules* **2017**, *50*, 137.

[29] S. Hotta, S. D. D. V Rughooputh, A. J. Heeger, F. Wudl, *Macromolecules* **1987**, *20*, 212.

[30] J. D. Yuen, A. S. Dhoot, E. B. Namdas, N. E. Coates, M. Heeney, I. McCulloch, D. Moses, A. J. Heeger, *J. Am. Chem. Soc.* **2007**, *129*, 14367.

[31] C. Enengl, S. Enengl, S. Pluczyk, M. Havlicek, M. Lapkowski, H. Neugebauer, E. Ehrenfreund, *ChemPhysChem* **2016**, *17*, 3836.

[32] D. Beatrup, J. Wade, L. Biniek, H. Bronstein, M. Hurhangee, J.-S. Kim, I. McCulloch, J. R. Durrant, *Chem. Commun.* **2014**, *50*, 14425.

[33] S. Chen, Y. Zhao, A. Bolag, J. Nishida, Y. Liu, Y. Yamashita, *ACS Appl. Mater. Interfaces* **2012**, *4*, 3994.

[34] S. Alem, S. Wakim, J. Lu, G. Robertson, J. Ding, Y. Tao, *ACS Appl. Mater. Interfaces* **2012**, *4*, 2993.

[35] Y. Jing, Y. Liang, S. Gheytani, Y. Yao, *Nano Energy* **2017**, *37*, 46.

[36] N. Y. Doumon, G. Wang, R. C. Chiechi, L. J. A. Koster, *J. Mater. Chem. C* **2017**, 6611.

[37] M. J. Frisch, G. W. Trucks, H. B. Schlegel, G. E. Scuseria, M. A. Robb, J. R. Cheeseman, G. Scalmani, V. Barone, B. Mennucci, G. A. Petersson, H. Nakatsuji, M. Caricato, X. Li, H. P. Hratchian, A. F. Izmaylov, J. Bloino, G. Zheng, J. L. Sonnenberg, M. Hada, M. Ehara, K. Toyota, R. Fukuda, J. Hasegawa, M. Ishida, T. Nakajima, Y. Honda, O. Kitao, H. Nakai, T. Vreven, J. A. Montgomery, J. E. Peralta, F. Ogliaro, M. Bearpark, J. J. Heyd, E. Brothers, K. N. Kudin, V. N. Staroverov, R. Kobayashi, J. Normand, K. Raghavachari, A. Rendell, J. C. Burant, S. S. Iyengar, J. Tomasi, M. Cossi, N. Rega, J. M. Millam, M. Klene, J. E. Knox, J. B. Cross, V. Bakken, C. Adamo, J. Jaramillo, R. Gomperts, R. E. Stratmann, O. Yazyev, A. J. Austin, R. Cammi, C. Pomelli, J. W. Ochterski, R. L. Martin, K. Morokuma, V. G. Zakrzewski, G. A. Voth, P. Salvador, J. J. Dannenberg, S. Dapprich, A. D. Daniels, Farkas, J. B. Foresman, J. V Ortiz, J. Cioslowski, D. J. Fox, Gaussian 09, Revision B.01. *Gaussian 09, Revis. B.01, Gaussian, Inc., Wallingford CT* **2009**.

Keywords: Organic bioelectronics, organic electrochemical transistors, organic semicoductors, quinones, stability.

Redox-stability of alkoxy-BDT copolymers and their use for organic bioelectronic devices

Alexander Giovannitti,, Karl J. Thorley, Christian B. Nielsen, Jun Li, Mary J. Donahue, George G. Malliaras, Jonathan Rivnay and Iain McCulloch*

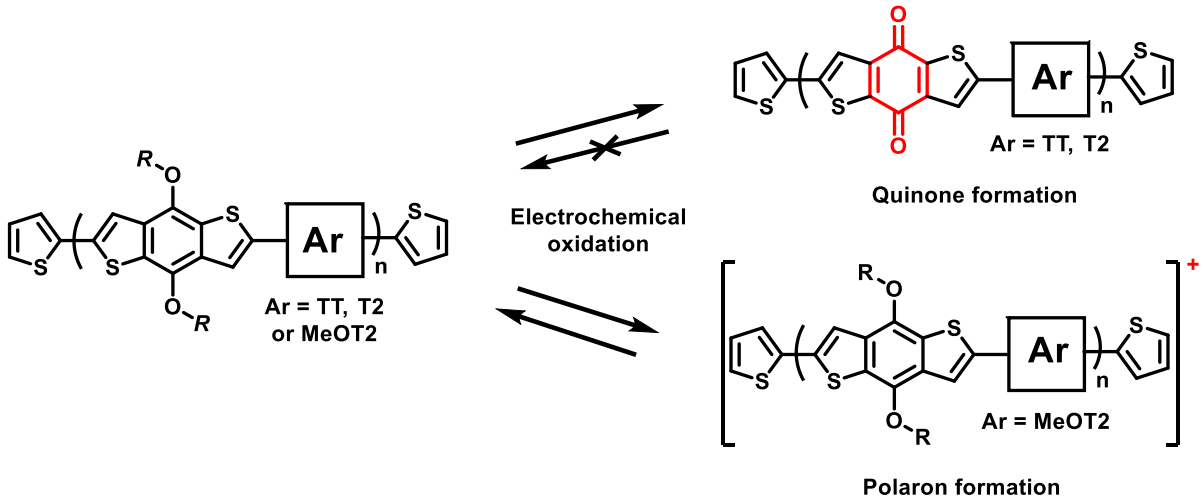

TOC